

Preliminary study of the effects of ageing on the long-term performance of NPP pipe

Salvatore Angelo Cancemi, Rosa Lo Frano^{*}

DICI-Università di Pisa, Pisa, Italy

ARTICLE INFO

Keywords:

Safety
Inverse method
Long-term operation
Ageing
Thermal loads
Maintenance

ABSTRACT

Most of today's operating nuclear plants are facing long-term operation (LTO) issues caused by the time degradation and/or deterioration suffered by the system, structure, and components (SSCs). These phenomena are known as ageing and are responsible for the change of material properties and, in turn may affect the structural integrity of plant SSCs.

The paper deals with the analysis of the performance of a primary pipe of a typical PWR subjected to ageing mechanisms. To the aim an inverse space marching method is applied. From reconstructed temperature it is possible to determine e.g. temperature values at surfaces that are difficult to reach and inspect. Accordingly, based on the thermal gradient across the pipe wall, the residual thickness of the pipe may be determined and used for structural capacity verification. Analytical and numerical (thermo-mechanical) analyses are performed considering several thinning rates. The effects of both homogeneous and heterogeneous thinning are also investigated.

The results suggest that an excessive (general or local) thinning may affect the strength capacity of pipe. The performance of the pipeline confirms the possibility of the life extension if the thinning rate is kept below 0.5 mm/year, even when the plant operating conditions are outside the prescribed operating limits.

1. Introduction

Most systems, structures and components (SSCs) of the nuclear plants were designed for 30–40 years of operation, and could be inadequate for service beyond the original design life or long-term operation (LTO). A lot of efforts has been spent identifying the main problems that mostly affect the behaviour of such plants and the consequences they may cause with the aim to systematically monitor, assess and control degradation effects that might compromise safety functions of the plant.

The IAEA NP-T-3.24 (IAEA, 2017) also refers to the term 'ageing' to describe "the continuous time dependent degradation of SSC materials ..." during normal service and transient conditions. As the components age, the plant original design ages too; this means that cumulative effects of ageing and obsolescence on the safety of nuclear power plants must be re-evaluated periodically to verify components (single component at small or whole plant at large (IAEA, 2003)) performances are within acceptable limits. To that purpose accurate evaluation of the aging effects on through state-of-art models and application of the aging-management software is needed. In doing that, descriptive, operating and functional information and data and stressors have to be

defined/determined. Fig. 1 shows the decrease of the safety margin as a function of the time: analysing it, it is clear how important it is to guarantee a minimum safety level, whatever the events that could occur. The existence of such level assures the safety margin at all times.

Aging analyses is performed and presented in this study to quantify the effect of the extended operation period on the structural integrity of Class I SSC. Specifically, the thermo-mechanical performance of a primary pipe of a 2nd Generation PWR is carried out considering the thermal degradation phenomena and the thinning (Electric Power Research Institute, 2002; Choi and Kang, 2000; Dooley and Chexal, 2000).

Thinning (homogeneous or localized-heterogeneous), due to the operation of the nuclear plants, determines a progressive reduction (few tens of μm per year) of the thickness of the pipe. If the thickness is reduced too much, the pipe may collapse under the internal pressure (Lo Frano and Forasassi, 2008, 2009; bib_Lo_Frano_and_Forassasi_2008; bib_Lo_Frano_and_Forassasi_2009).

In monitoring the progression of the thinning, the electrical analogue may be used to quantify and predict the progression of the degradation. Since the temperature is the potential, or driving, function for the heat flow and the thermal resistance is dependent on the

^{*} Corresponding author.

E-mail address: rosa.lofrano@ing.unipi.it (R. Lo Frano).

Nomenclature		T_{∞}	Fluid temperature [$^{\circ}\text{C}$]
AT	Accelerated Corrosion	x	Input signal
C	Convolution coefficient	y	Output signal
c	Heat capacity [$\text{J kg}^{-1}\text{K}^{-1}$]	Z	Smoothed measured temperature [$^{\circ}\text{C}$] at time step t
FAC	Flow acceleration corrosion	<i>Greek symbols</i>	
F_o	Fourier number for 1D problem	ρ	Density [kg m^{-3}]
HTC	Heat transfer coefficient [$\text{W m}^{-2}\text{K}^{-1}$]	σ	Stress [Pa]
k	Thermal conductivity [$\text{W m}^{-1}\text{K}^{-1}$]	α	Li thermal expansion [$^{\circ}\text{C}^{-1}$]
L_r	Residual Life of component [y]	$\Delta r, \Delta \varphi$	Radial and circumferential length [m]
LTO	Long Term Operation [y]	ν	Poisson's ratio [-]
M	Number of the point in the average [-]	<i>Subscripts and superscripts</i>	
p_i	Pressure at internal radius r_i [Pa]	i	Spatial node index
p_o	Pressure at radius r_o [Pa]	inn	Inner location in the pipe
q	Heat flux [W m^{-2}]	mid	Middle location in the pipe
r	Radius [m]	min	Minimum
r_{in}	Inner radius [m]	red	Reduced
r_{mid}	Intermediate radius [m] with $n = 1, 2 \dots 5$	sr	Requirement
r_{out}	Outer radius [m]	out	Outer location in the pipe
SOL	Service Operation Life [y]	j	Temporal node index
t	Time [s]	∞	Ambient
t_o	Beginning of life [y]	n	1,2,3,4,5 different radius length
T	Temperature [$^{\circ}\text{C}$]		

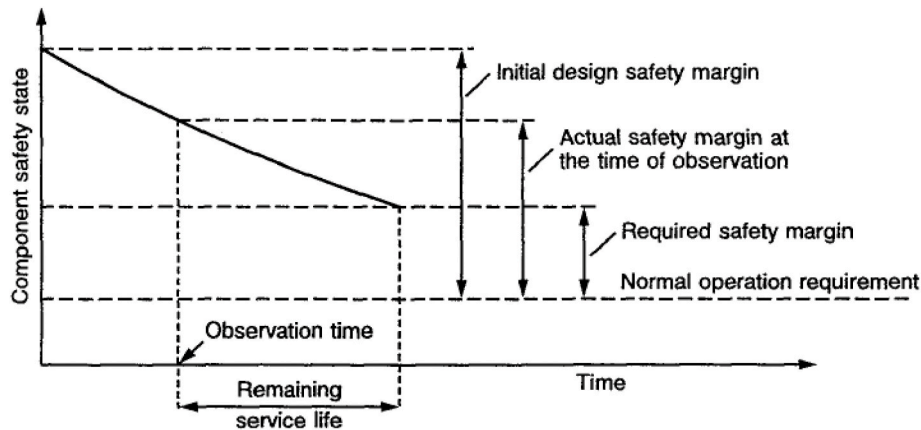


Fig. 1. Conceptual component safety state.

thermal conductivity, thickness of material and area, the thickness reduction, caused by the aging, can be determined based on the temperature gradient across the wall thickness (Hetnarski and Eslami). Consequently, it will be possible to verify the structural capacity of the pipe, according to ASME III sect. NB-3232 (ASME, 1980) for its actual thickness value.

The remaining pipe service life is so dependent on the minimum thickness requirement and thinning rate. In doing that, the heat inverse problem, allowing to reconstruct the temperature gradient based on the external temperature of the pipe, plays an important role as well as for thinning investigation purposes, the knowledge of the annual rate of erosion/corrosion of the pipe (data obtained from material specifications).

In the following, the methodological approach used to determine stressors will be described as well as the application of the inverse method to solve the heat transfer problem. The numerical analysis of aged pipe for several thinning type and rate is presented and discussed in Section 3.

2. Thinning investigation

Large and long-life passive structure and components, such as pressure vessels, concrete structures, and pipe, are the most critical to assess in terms of safety and performance, this assessment is made even more difficult due to the lack of (in-depth) knowledge of aging phenomena and mechanisms. Therefore, to deal with the gap that characterizes the design of the actual SSCs of the existing plants, a design verification that considers the most demanding aspects of aging, in form of basic assumptions and/or input data, must be made.

In this paper, a straight LWR pipe is analysed as it is one of the major plant subsystems significantly that may be affected by ageing phenomena (see IAEA Tech Doc 540). Primary pipe shall be designed for the most severe condition of internal pressure and temperature allowed, and transient loadings. The nominal minimum thickness of a pipe wall, required for design pressure and for temperature not exceeding those for the various materials, is:

$$t_m = \frac{pD_o}{2(SE + Py)} + A \quad (1)$$

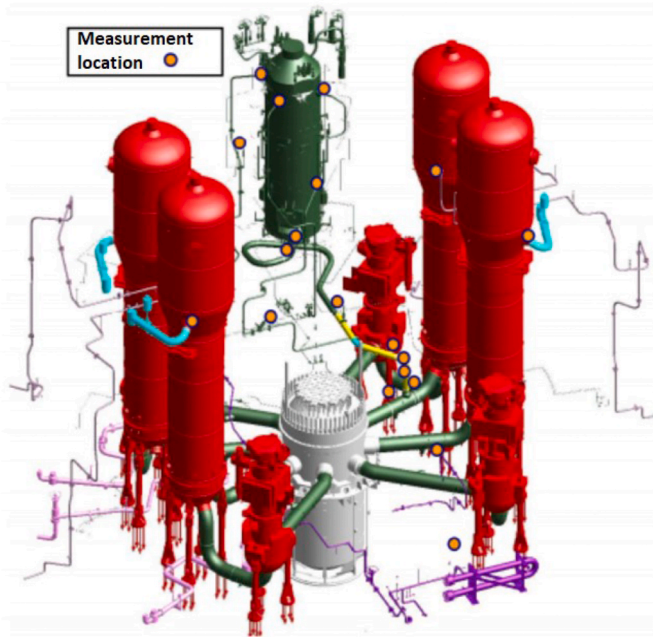


Fig. 2. Scheme of sensors location (orange points) to monitor and control the primary system operation as in (Cancemi and Lo Frano, 2020).

Where t_m is the minimum thickness, p is the internal design pressure, D_0 the outside diameter of pipe. SE is the maximum allowable stress in material at the design temperature, y is a numerical coefficient and A is the additional thickness to be consistent with the expected life of the pipe.

As aforementioned, based on the knowledge of the temperature gradient across the pipe wall it could be possible to determine the actual thickness value, and verify the bearing capacity of the pipe itself for LTO condition. The methodology to investigate the thermo-mechanical performance of a PWR pipe is consisting of:

- 1) reconstruction of temperature profile by inverse technique;
- 2) determination of all thermal and mechanical loadings;
- 3) identification of aging phenomena affecting the pipe;
- 4) thermo-mechanical analysis;

In this study the thinning, which may ultimately cause perforation of the pipe wall if allowed to continue indefinitely, and the thermal degradation are considered as main aging phenomena. The former occurs throughout the affected region, rather than in a localized area as in the case of pitting or cracking, and is proportional to: temperature, material, flow velocity, etc. The latter depends on the time and temperature of exposure, together with the material type and its chemical composition.

In this assessment, several wall-thinning rates and time-temperature dependent material property were considered (Matsumura, 2015).

The stress to calculate (σ_r , σ_θ and σ_z) for verification of load bearing capacity, for both steady and transient temperature distributions, are dependent on the mechanical and thermal loads and are expressed in cylindrical coordinate system as:

$$\sigma_r = \frac{E}{(1-\nu)} \left\{ -\frac{1}{r^2} \int_{r_i}^r \alpha T r dr + \frac{r^2 - r_i^2}{r^2 (r_0^2 - r_i^2)} \int_{r_i}^{r_0} \alpha T r dr \right\} + \frac{(p_i r_i^2 - p_0 r_0^2)}{r_i^2 - r_0^2} - \frac{1}{r^2} \frac{(p_i - p_0) r_0^2 r_i^2}{r_0^2 - r_i^2} \quad (2)$$

$$\sigma_\theta = \frac{E}{(1-\nu)} \left\{ \frac{1}{r^2} \int_{r_i}^r \alpha T r dr + \frac{r^2 + r_i^2}{r^2 (r_0^2 - r_i^2)} \int_{r_i}^{r_0} \alpha T r dr - \alpha T \right\} + \frac{p_i r_i^2 - p_0 r_0^2}{r_0^2 - r_i^2} + \frac{(p_i - p_0) r_0^2 r_i^2}{r^2 (r_0^2 - r_i^2)} \quad (3)$$

$$\sigma_z = \frac{E}{(1-\nu)} \left\{ \frac{2\nu}{(r_0^2 - r_i^2)} \int_{r_i}^{r_0} \alpha T r dr - \alpha T \right\} \quad (4)$$

Where E is the Young modulus, α is the linear expansion coefficient, ν is the Poisson's coefficient, and r is the radial direction along which heat flows. r_i and r_0 are the inner and outer radius of pipe, respectively, and T is the temperature. The stress σ_z is independent from the pressure. From the above equations, it is easy to understand that, for an adequate evaluation of the pipe performance, it is necessary to determine the temperature.

2.1. The inverse heat transfer problem

The inverse heat transfer problem (IHTP) is used to determine the internal temperature of pipe (Becket et al., 1995; Taler et al., 2011) starting from the known physical parameters characterizing the component's operation. It is a control method for monitoring thermal stresses and pressure-caused stresses and hence the status pressure components. Moreover, since it is based on the elaboration of known experimental data (e.g. temperature of the internal pipe surface), to cope with the instabilities, mainly errors and noising, a suitable and reliable filtering/tuning technique of proven reliability (Cancemi and Lo Frano, 2020) has been implemented. This made it possible to obtain a stable output signal. Although the method is not new in literature, it is the first time that it is used in combination with FEM investigation to analyse the safety performance of an aged pipe. The studies available in the open literature are mainly focused on the thermal analysis (1D or 2D) of pipe and on the description of the way temperature at the inner surface is monitored and acquired. As indicated in (Cancemi and Lo Frano, 2020), IHTP is used because or when direct measurements are not possible, specifically, at the pipe inner surface. Wikstrom et al. (Wikstrom et al., 2007) studied in fact the heat transfer modes of a steel slab and proposed an approach to determine the time history of (local) temperature and heat flux based on the knowledge of the temperature inside the slab.

Taler et al. (Taler et al., 2011) applied the finite element method (FEM) to calculate stress for pressure components with complex geometry, once the influence function is known. Okamoto and Li (Okamoto et al., 2007) instead investigated the unidirectional solid-liquid interface of a solidification system by means of similar method. Finally, Luet et al. (2010) investigated the performance of a 2-D elbow pipe section subjected to an unknown transient fluid temperature (Luet et al., 2010), correlating the accuracy of the measured signal, i. e. indirect temperature, to noising.

2.1.1. Reconstruction of temperature: approach description and application

The approach used to reconstruct temperature trends is based on the acquisition and processing of the temperature values: thermocouples installed on the outer surface of the pipeline allowed to provide the external temperature, with a sampling rate of e.g. 1 Hz. The elaborated signal by monitoring system is used for the assessment of thermal loads (e.g. bulk temperature in the pipe) (Miksch and Schucktan, 1990). Online monitoring of operational parameters allows to control the plant operation. Example of such a system is shown in Fig. 2.

The inverse space marching method is then applied, as shown in Fig. 3, to numerically calculate the internal temperature (T). Smoothing of the measured temperature histories is necessary due to the fact that the monitoring system may skip data points when the temperature variation is below 0.5 °C. To minimize noising, the Savitzky-Golay's

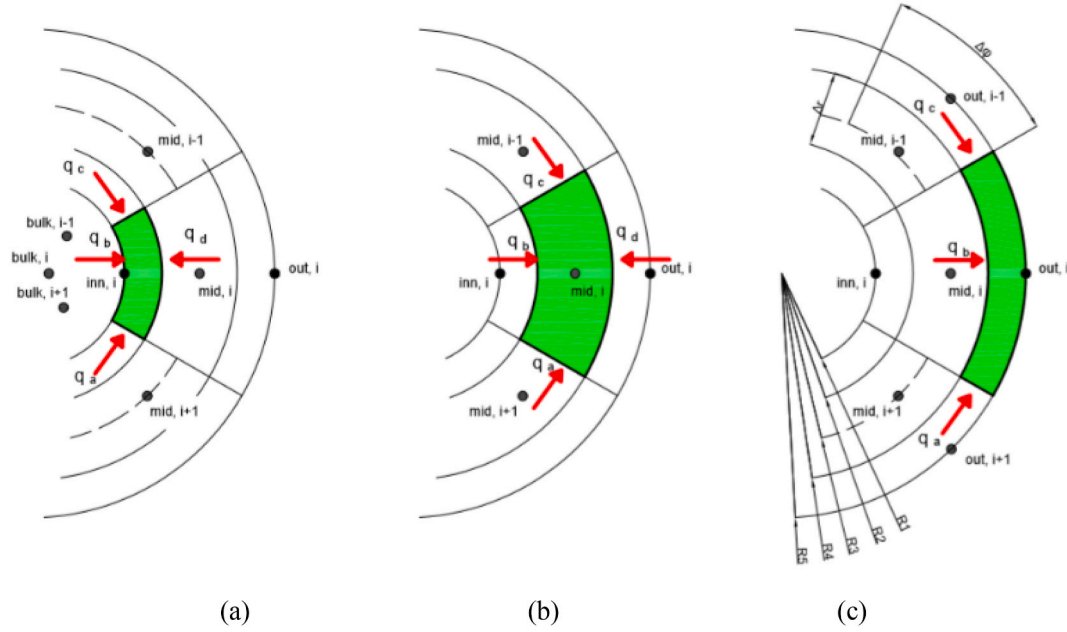


Fig. 3. Pipe wall layering for the application of control volume method. Moving rightward they show the heat balance at inner node (a), at the middle node (b) and at the outer node (c).

filter, which is new respect with the Gram's polynomials approach used by Taler et al., 1995 (Al-Khalidy, 1998; Taler, 2011), was implemented in the developed Matlab tool (Cancemi and Lo Frano, 2020).

The method marches in space towards the inner surface of the pipe cross-section by using the energy balance equations to determine the temperatures in adjacent nodes.

In this study, the pipe cross section is divided into the three finite volumes (green coloured boxes) shown in the schematization of Fig. 3.

$$T_{inn,i} = T_{out,i} + \left[\frac{(r_4^2 - r_2^2)}{r_2} + (r_5^2 - r_4^2) \left(\frac{1}{r_4} + \frac{1}{r_2} \right) \right] \frac{\Delta r}{2a} \frac{dT_{out,i}}{dt} + \frac{(\Delta r)^2 (r_5^2 - r_4^2) (r_4^2 - r_2^2)}{4\alpha^2 r_2 r_4} \frac{d^2 T_{out,i}}{dt^2} \quad (8)$$

In the node "i" at inner surface of the inner volume, the heat balance equation is:

$$c\rho \frac{\Delta\phi}{2} (r_5^2 - r_4^2) \frac{dT_{inn,i}}{dt} = q_a \frac{\Delta r}{2} + q_b \Delta\phi r_4 + q_c \frac{\Delta r}{2} + q_d \Delta\phi r_2 = k \frac{T_{inn,i+1} - T_{inn,i}}{\Delta\phi r_1} \frac{\Delta r}{2} + q_{inn,i} \Delta\phi r_1 + k \frac{T_{inn,i-1} - T_{inn,i}}{\Delta\phi r_1} \frac{\Delta r}{2} + k \frac{T_{mid,i} - T_{inn,i}}{\Delta r} \Delta\phi r_2 \quad (9)$$

Because of thin and long pipe assumption, the energy balance equations in cylindrical coordinates are solved in 1D. The temperature is so determined for each volume (inwards radial direction) in its nodes, and in particular for the node "i" of the outer surface of the volume shown in Fig. 3 (c) it is given as:

$$c\rho \frac{\Delta\phi}{2} (r_5^2 - r_4^2) \frac{dT_{out,i}}{dt} = q_a \frac{\Delta r}{2} + q_b \Delta\phi r_4 + q_c \frac{\Delta r}{2} = k \frac{T_{out,i+1} - T_{out,i}}{\Delta\phi r_5} \frac{\Delta r}{2} + k \frac{T_{mid,i} - T_{out,i}}{\Delta r} \Delta\phi r_4 + k \frac{T_{out,i-1} - T_{out,i}}{\Delta\phi r_5} \frac{\Delta r}{2} \quad (5)$$

From Eq. (2) it is possible to calculate the temperature at the centre of the cross section (Fig. 3 (b)) ($T_{mid,i}$) as:

$$T_{mid,i} = T_{out,i} + \frac{\Delta r (r_5^2 - r_4^2)}{2\alpha r_4} \frac{dT_{out,i}}{dt} \quad (6)$$

As before, by applying the energy balance it is possible to calculate the temperature at the node "i" of the inner surface of the internal volume of the pipe section ($T_{inn,i}$):

$$T_{inn,i} = \frac{\Delta r}{2\alpha r_2} (r_4^2 - r_2^2) \frac{dT_{mid,i}}{dt} + \left(1 + \frac{r_4}{r_2} \right) T_{mid,i} - \frac{r_4}{r_2} T_{out,i} \quad (7)$$

Eq. (7) can be expressed also in terms of $dT_{out,i}/dt$ in order to directly correlate the internal and external superficial pipe temperature as:

Finally, the heat flux is evaluated from Eq. (9) as:

$$q_{inn,i} = k \left[\frac{(r_2^2 - r_1^2)}{2\alpha r_1} \frac{dT_{inn,i}}{dt} - \frac{r_2}{r_1} \frac{(T_{mid,i} - T_{inn,i})}{\Delta r} \right] \quad (10)$$

Assuming constant heat transfer coefficient (h_i) and heat transfer coefficient at the inner surface of the internal volume (h_i), therefore the heat flux ($q_{inn,i}$) is obtained as:

$$q_{inn,i} = h_i (T_{\infty,i} - T_{inn,i}) \quad (11)$$

In the above Eq. (11), the bulk temperature ($T_{\infty,i}$) of fluid is given as:

$$T_{\infty,i} = T_{inn,i} + \frac{k}{h_i} \frac{(r_2^2 - r_1^2)}{2\alpha r_1} \times \left\{ \frac{dT_{out,i}}{dt} + \left[\frac{(r_4^2 - r_2^2)}{r_2} + (r_5^2 - r_4^2) \left(\frac{1}{r_4} + \frac{1}{r_2} \right) \right] \frac{\Delta r}{2a} \frac{d^2 T_{out,i}}{dt^2} + \frac{(\Delta r)^2 (r_5^2 - r_4^2) (r_4^2 - r_2^2)}{4\alpha^2 r_2 r_4} \frac{d^3 T_{out,i}}{dt^3} \right\} + \frac{k}{h_i} \frac{r_2}{r_1} \frac{(T_{mid,i} - T_{inn,i})}{\Delta r} \quad (12)$$

In Eq. (12) the high orders of time-derivative affect only the signal at outer wall node.

Finally, a smoothing technique, i.e. via Savitzky-Golay filter, has to be/is used before the evaluation of the temperature at the different nodes in order to minimize noising or measurement errors, which could otherwise cause large oscillations in determining $T_{\infty,i}$. In addition,

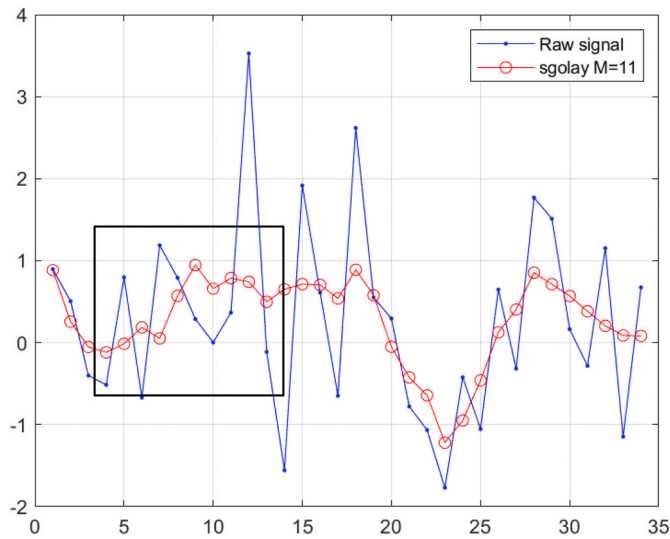


Fig. 4. Representation of 11-point moving polynomial smooth (polynomial order 3rd): the blue points represent the experimental data; the red points represent the calculated data. For the temperature signal the unit system are the temperature [° C] on the order axis and the time [s] on the abscissa.

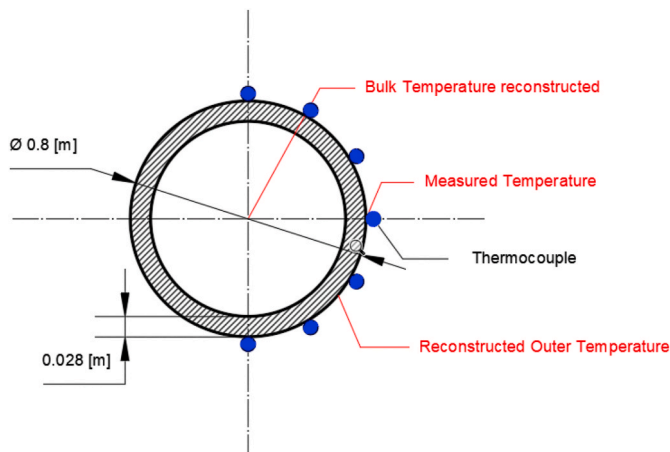


Fig. 5. Pipe cross-section.

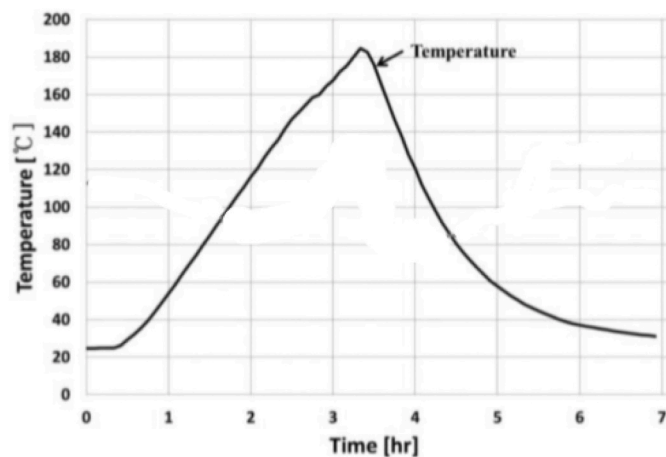


Fig. 6. Input temperature plot for IHCP inverse approach (Se-Beomet al., 2019).

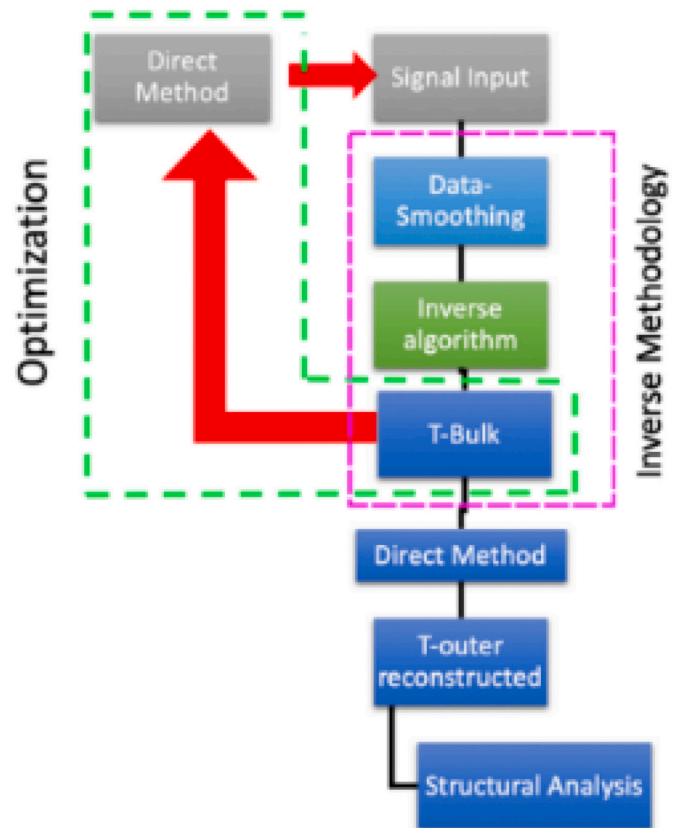


Fig. 7. Inverse Methodology diagram.

temperatures obtained from the IHCP, using the CVM, were compared with those from the direct heat conduction problem (DHCP) in order to validate the code.

The selected Savitzky-Golay (SG) filter (Savitzky and Golay, 1964) is based on the least squares polynomial fitting across a moving window within the data in the time domain. It permits to minimize the least-squares error in fitting a polynomial to frame of noisy data. In the developed code tool, it was implemented through the equation:

$$Z_j = \sum_{i=-\frac{M-1}{2}}^{\frac{M-1}{2}} C_i y_{j+i} \tag{13}$$

with $\frac{M-1}{2} \leq j \leq n - \frac{M-1}{2}$.

In Eq. (13) M , $x[j]$, $y[j]$ are respectively the number of the points in the average ($j = 1, 2 \dots n$), the input and output signal. C_i are the convolution coefficients. As the window moves with a size M , the filter gives back a new experimental point of the experimental n -points treated signal. An application example for a cubic polynomial is shown in Fig. 4.

In this study, the IHCP inverse approach was applied to the pipe cross section of Fig. 5. The input temperature was from the Se-Beomet's study (Se-Beomet al., 2019) (Fig. 6) while the SG's filter was used to smooth and replace data (since of polynomial order and window size). The applied procedure, schematized in the diagram of Fig. 7, consists of:

- 1) The experimental data are linearly interpolated so to obtain the outer temperature trend;
- 2) The interpolated data-points are smoothed by the SG's filter;
- 3) The smoothed signal is used as input for the inverse algorithm to reconstruct bulk temperature profile;
- 4) Determination of the external temperature and, accordingly, stress at the inner and outer surface of the pipe by solving the direct heat

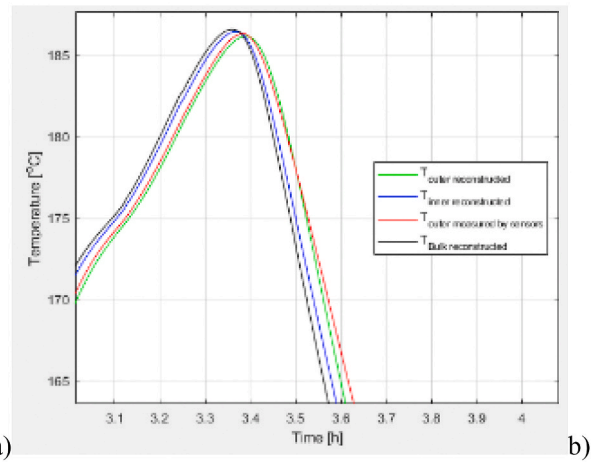
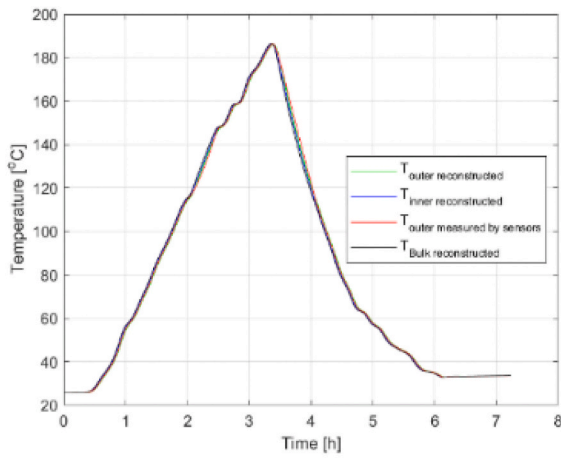


Fig. 8. a) Smoothed temperature trend for $M = 13$. In b) is shown the local zoom of the temperature peak.

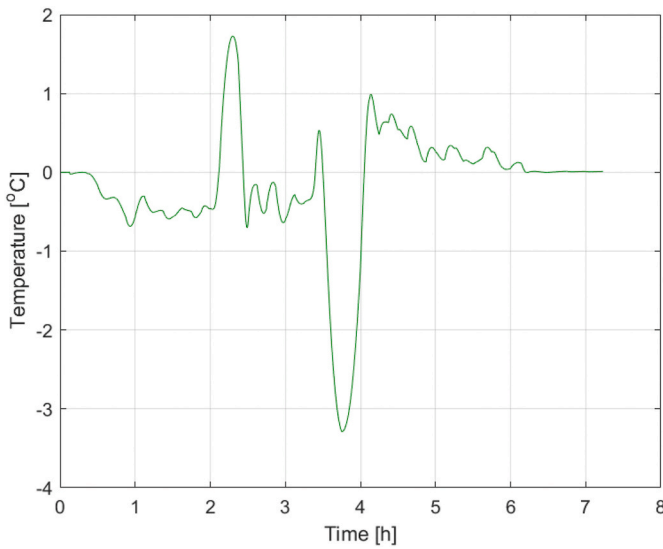


Fig. 9. Error in reconstructing data.

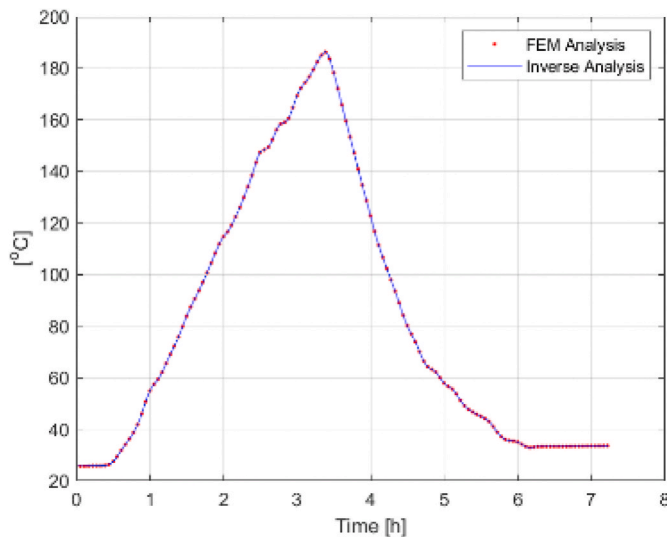


Fig. 10. Trend of the outer reconstructed temperature: FEM vs CVM.

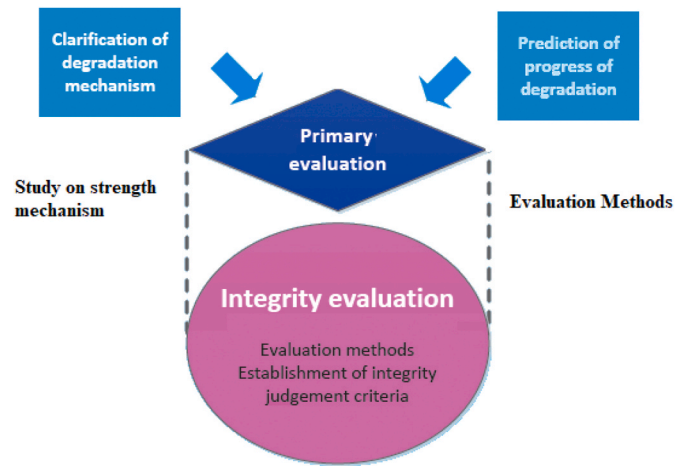


Fig. 11. Ageing effects assessment.

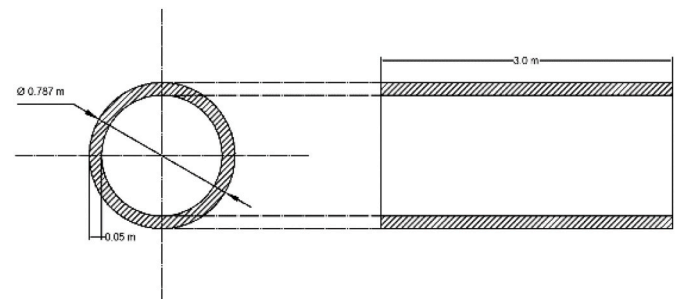


Fig. 12. Cross section of pipe: geometry of FE model.

transfer problem, once known the bulk temperature; Indeed, the “measured stresses” are obtained from the experimental data, while the “generated stresses” from the direct algorithm.

2.1.2. Reconstruction of temperature: results

The window sizes M chosen in this study are: $M = 9$, $M = 11$, $M = 13$, $M = 21$, $M = 31$. To select the suitable window length M of SG filter, the generated stress is considered as reference signal. By comparing the smoothed measured temperature, for different M , with the reference one, it was possible to identify that the best filter windows capable to

Table 1
Residual pipe wall thickness allowing the extension of life.

Plant Life[y]	Residual pipe thickness ($t_{nom} - W_r$) [cm]			
	$W_r=1.5$	$W_r=1.15$	$W_r=0.7$	$W_r=0.5$
10	3.5	3.85	4.3	4.5
20	2	2.7	3.6	4
30	0.5	1.55	2.9	3.5
40	-	0.4	2.2	3
50	-	-	1.5	2.5
60	-	-	0.8	2

Table 2
Residual life (L_r) beyond 30 years operation vs structural strength decrease.

Residual Life [y]	Yielding Strength [% nominal value]			
	$W_r=0.5$	$W_r=0.7$	$W_r=1.15$	$W_r=1.5$
15.72	2.66	-	-	100
12.76	0.55	-	-	95
9.46	-	-	-	90
5.76	-	-	-	85
1.57	-	-	-	80

assure a high level of accuracy of the method are $M = 9$, $M = 11$ and $M = 13$ (Fig. 8). These represent the best code setup as the maximum error in reconstructing data was between $+1.7^\circ$ and -3.29°C (see Fig. 9). The analysis of this case-study confirmed the consistency of the proposed methodology, and the accuracy of this new tool for which no other applications can be found in literature.

2.1.3. Validation of CVM

To validate the CVM a transient dynamic analysis was carried out assuming the same geometry (see Fig. 5) and material properties, and the same boundary and initial conditions. These latter were precisely the temperature trend of Fig. 6, and the pressure (i.e. 14 MPa).

Thermo-mechanical (finite element) analysis was carried out by MSC®Marc code (MSC Marc Help Documentation, 2019) on a steel pipe model, made of shell type elements with a non-zero curvature along the

middle surface and with a small thickness with respect to the curvature radii (Raju and Hinton, 1980). Material properties are varying with the temperature (ASME, 2019). Bilinear interpolation is used for the displacements and the rotations. Same thermal transient duration and sampling frequency of the acquired temperature signal (1 Hz) are assumed.

Fig. 10 shows the comparison between the FEM and CVM temperature trends.

Analysing them, it can be observed that they are almost superimposable confirming the reconstruction capability of the code implemented. It is to note that this is of great importance in the assessment of such a technique that could be adopted, when for technical reasons, it is not possible to install thermocouples directly at the internal pipe surface.

3. LTO pipe performance

The wall thinning is the consequence of the dissolution of the normally protective oxide layer from the surfaces of carbon and low alloy steel pipe. The wear rate depends on several parameters, some of the most important including the temperature and the hydrodynamics. Under single-phase conditions thinning was experienced in the temperature range from 80 to 230 °C, whereas between 140 and 260 °C under two-phase flow conditions.

When thinning mechanisms occur at local areas of pipe components, as shown in Yun et al. 2020 (Yunet al., 2020), degradation can cause eventually leaks or ruptures in the pressure boundary of nuclear power plants (NPPs). Reliable analyses to support inspection strategy become thus very important to prevent pipe rupture. The performed numerical assessment is based on the approach shown in Fig. 11.

In this section, FE analyses of second Generation PWR pipe of about 78 cm diameter and about 5 cm thickness are presented in order to verify if the thinning is capable of jeopardising the integrity of the primary system (Fig. 12). The results from the CVM as well as the loads from/representative of the nominal operation were inputted to FE model (external coupling between MARC and Matlab codes). The model boundary conditions were the vertical supports at the edge and at intermediate pipe length; the initial conditions were the temperature trend shown in the previous Fig. 6, and 14 MPa internal pressure. Material properties were assumed temperature dependent. A thermal expansion coefficient varying with the temperature was also imposed as well as the Von Mises criterion to measure the stress level.

Several thinning rates, e.g. from 0.5 to 1.5 mm/yr, as caused mainly by flow acceleration corrosion, were considered for the thermo-mechanical analyses. Band method is used to calculate wear rate of the pipe (NEA/OECD, 2014). In addition, both homogeneous and heterogeneous thinning was analysed. The effect of general pipe layout was

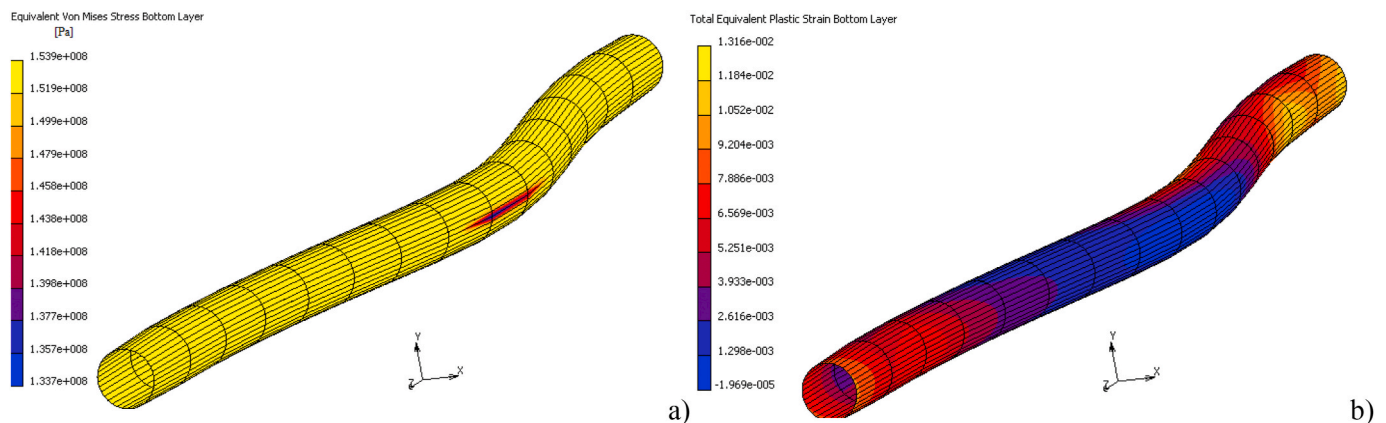


Fig. 13. a, b: Equivalent Von Mises stress (at the bottom layer) and the resulting plastic deformation (b) for localized and heterogeneous thickness reduction. The nominal pipe thickness, 30 yr aged, is $t_{nom} = 1.55$ cm (Table 1); while the section with localized thinning has $t_{reduced} = 0.8$ cm.

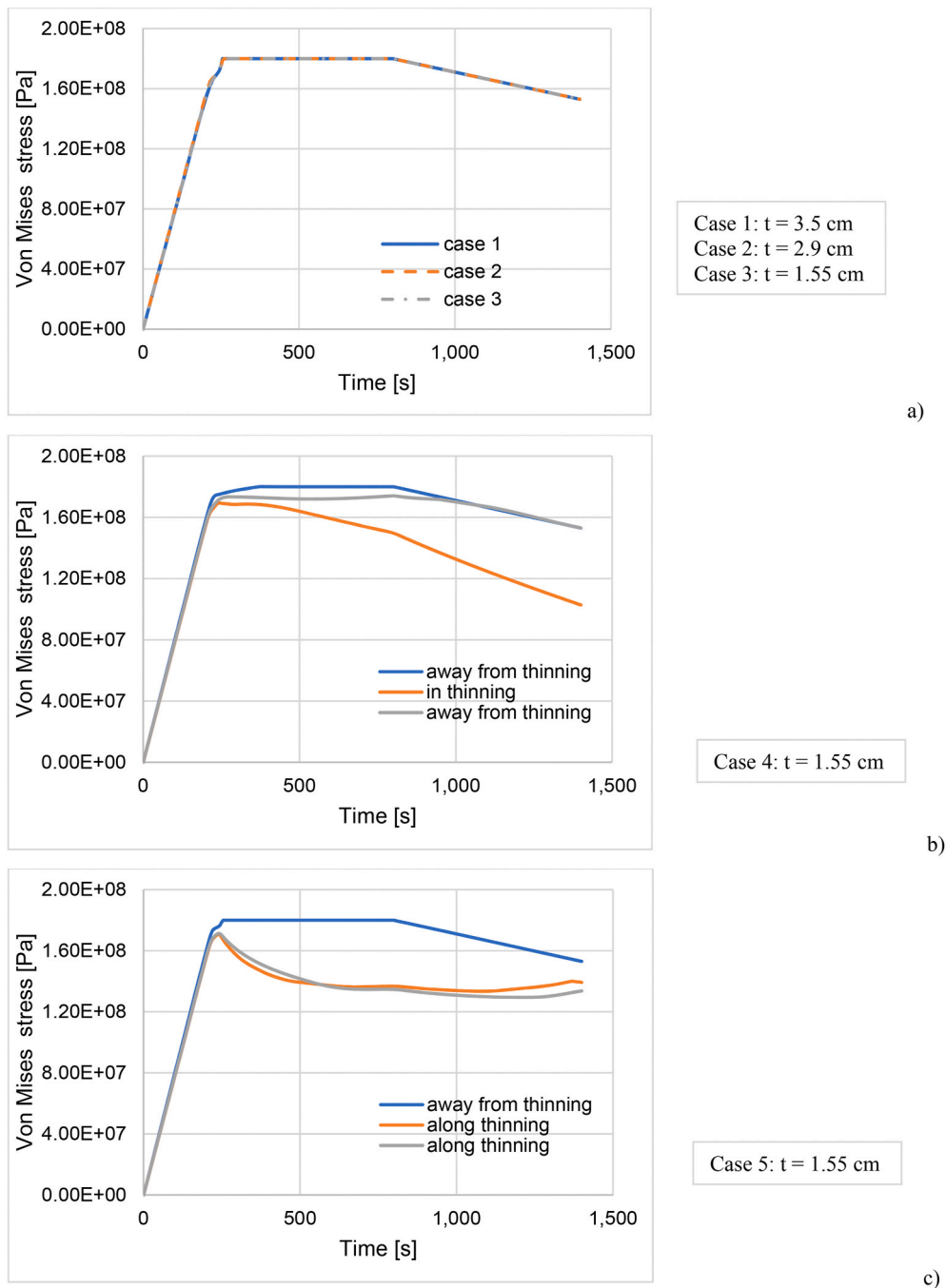


Fig. 14. a, b, c: Equivalent Von Mises stress (at the bottom layer) for pipe subjected to homogenous thinning (a) and thinning localized along a generatrix (b) and in a part of pipe (c). In these simulations, actual yielding strength is considered.

not investigated in this study.

It should be emphasized that thinning is not, in general, a mechanism that affects the internal surface of the pipe uniformly, as evidenced by the EPRI study (EPRI, 2006) and by Yun et al. 2016 (Yun et al., 2016), due to the liquid droplet impingement erosion, cavitation etc. Accordingly, it becomes more difficult to identify in time before it can cause/trigger an incidental scenario. For these reasons, the simulations carried out have considered both the ideal-theoretical case of homogeneous thinning of the thickness along the whole pipe and the case of thinning localized along one generatrix or only in a part of the pipe. The remaining service life of pipe (termed SOL in (NEA/OECD, 2014)) may be also calculated based on the knowledge of its minimum thickness (t_{min}), minimum thickness requirement (t_{sr}) and thinning rate (W_r) and

age (e.g. t_0+20 yr, t_0+30 yr; t_0+40 yr, where t_0 is the beginning of life) (Netto et al., 2007).

3.1. FE test results

In what follows the results of the performed transient thermo-mechanical (numerical) analyses are presented. The results show that long term operation of the pipe, beyond 30 years of operation, is still possible if the annual corrosion rate is kept lower than 0.7 mm/yr (Table 1). Moreover, as W_r decreases the life of pipe increases (green boxes in Table 1). It can also be observed that the residual life (L_r) of the pipe is dependent on the degradation of the material properties: assuming the same W_r , e.g. equal to 0.5 mm/yr, and for 20% reduction

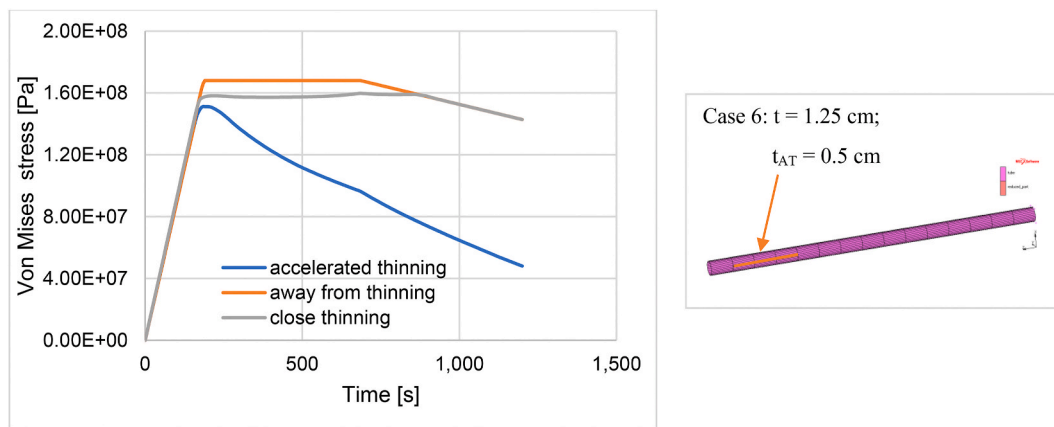


Fig. 15. Equivalent Von Mises stress (at the bottom layer) of pipe subjected to heterogeneous and accelerated thinning-AT- (orange coloured).

of the steel yielding strength the useful residual life passes from approximately 15.7 yr to about 1.5 yr (Table 2). Moreover, the red boxes indicate that the component should be replaced to not impair the safety of plant operation.

Analysing the results of Table 1 against the ASME criterion of “87.5% of nominal wall thickness” (used to determine whether continued operation is acceptable or if a repair or replacement has to be implemented prior to return to service) we can say that for $W_r \ll 0.5$ mm/yr the thickness component may be considered adequate for the service. Whether the residual wall thickness is below $0.875 t_{nom}$ (< 3.925 cm) a further (re)evaluation is required. Furthermore, the thermal gradient (ΔT) will increase in proportion to the ratio between the nominal thickness and the residual thickness of the pipe, in the case of normal operation hypothesis and for unchanged thermal conductivity, therefore, it is possible to control the pipe performance by monitoring the external temperature ($T_{out} = T_{int} + \Delta T$).

The generalised thinning involves throughout the surface of steel when a slow and uniformly distributed loss of material appears. However, this general degradation mechanism is not responsible of any appreciable localized deformation and/or damage. In Fig. 13 are shown the Equivalent von Mises stress and the resulting plastic deformation for localized thickness reduction: different deformations appear at the pipe surface caused by the localized thickness reduction up to 0.8 cm. They are mainly located in the areas of the maximum deflection where thinning degradation is worse (and could be even more because of the liquid droplets impingement).

By comparing the stress plots provided in Figs. 14 and 15, and taking into account that the pipe is subjected to the same Class I load combinations, it is possible to say that the structural integrity is assured even when heterogeneous thickness reduction, caused by accelerated ageing and premature degradation, occurs.

4. Conclusion

By coupling the inverse space marching method to verify the capability of a PWR primary, aged pipe, the thermo-mechanical analysis demonstrates that the pipe retains the required safety margin for long term operation.

The thermal analogue seems to be a suitable method to control the progression of thinning by controlling and reconstructing the internal temperature of the pipe.

The FEM analyses allowed to determine the pipe capacity of guaranteeing the operating conditions for different rate and type (localized or generalised) of thinning.

In summary, the carried-out analyses have highlighted:

- For $W_r = 0.5$ mm/y and strength reduction (80% nominal value), the useful life of the component decreases approximately of 20%.
- The thermal gradient increases in proportion to the ratio between the nominal thickness and the residual thickness of the pipe. Consequently, it is possible to control the pipe degradation and performance by monitoring the external pipe surface temperature.
- Slow and uniformly generalised thinning involving throughout the surface of steel pipe is not responsible of any appreciable localized deformation and/or damage. The opposite happens for localized thinning, particularly for the heterogeneous one, that is characterised by flexural effects that become more and more marked as time passes and thinning progresses. Bending deformation modes appears along the length of pipe generatrix (see Fig. 13 b).
- Even when the PWR operating conditions (e.g. temperature, pressure, water chemistry) are outside the prescribed operating limits, if W_r is less than 0.5 mm/y, the pipe perforation could be avoided for another 30 years of normal operation (LTO of 60 y) in the absence of other factors that could further degrade the pipe performance.

Finally, it is worthy to remark that the thinning of steel pipe and related components is a continuous and almost irreversible process, for this reason, timely feedbacks coming from experience and assessment (implementation of effective management programmes) are essential to prevent unacceptable ageing degradation that could jeopardise the plant integrity.

Credit author statement

Conceptualization; Methodology, Writing - Original Draft and Funding acquisition: Rosa Lo Frano. Writing - Review & Editing and Software: Salvatore A. Cancemi. Writing - Review & Editing: Rosa Lo Frano and Salvatore A. Cancemi.

Declaration of competing interest

The authors declare that they have no known competing financial interests or personal relationships that could have appeared to influence the work reported in this paper.

Acknowledgement

The paper has been carried out in the framework of NARSIS (New Approach to Reactor Safety Improvements) H2020 EU Project (Grant Agreement No. 755439), which has received funding from the Euratom research and training programme 2014–2018.

References

- Al-Khalidy, N., 1998. On the solution of parabolic and hyperbolic inverse heat conduction problems. *Int. J. Heat Mass Tran.* 41, 3731–3740.
- ASME III, 1980. Division 1 – Subsection NB-3232, ASME, Boiler and Pressure Vessel Committee.
- ASME, 2019. BPVC 2010 Sec. II Part D Properties.
- Beck, J., et al., 1995. *Inverse Heat Conduction Problems: III Posed Problems*. Wiley, New York.
- S.A. Cancemi and R. Lo Frano, *Inverse Heat Conduction Problem in Estimating NPP Pipeline Performance - Proceedings of ICONE-28th International Conference on Nuclear Engineering August 2-6, 2020, Anaheim, USA*.
- Choi, Y.H., Kang, S.C., 2000. Evaluation of piping integrity in thinned main feedwater pipes. *Nucl. Eng. Technol.* 32, 67–76.
- Dooley, R.B., Chexal, V.K., 2000. Flow-accelerated corrosion of pressure vessels in fossil plants. *Int. J. Pres. Ves. Pip.* 77, 85–90.
- Electric Power Research Institute (EPRI), 2002. TR-106611-R1, *Flow Accelerated Corrosion in Power Plants*.
- EPRI, 2006. Chug Position paper No8, *Determining Piping Wear Caused by Flow-Accelerated Corrosion from Single-Outage Inspection Data*.
- R. B. Hetnarski, M.R. Eslami. *Thermal Stresses – Advanced Theory and Applications*. II Ed. Springer.
- IAEA, 2003. *Assessment and Management of Ageing of Major Nuclear Power Plant Components Important to Safety - Primary Piping in PWRs*. IAEA-TECDOC-1361.
- IAEA, 2017. *Handbook on Ageing Management for Nuclear Power Plants*. NP-T-3.24.
- Lo Frano, R., Forasassi, G., 2008. Buckling of imperfect thin cylindrical shell under lateral pressure. *Sci. Technol. Nucl. Instal.* 685805.
- Lo Frano, R., Forasassi, G., 2009. Experimental evidence of imperfection influence on the buckling of thin cylindrical shell under uniform external pressure. *Nucl. Eng. Des.* 239 (2), 193–200.
- Lu, T., et al., 2010. A two-dimensional inverse heat conduction problem in estimating the fluid temperature in a pipeline. *Appl. Therm. Eng.* 30, 1574–1579.
- MSC Marc Help Documentation, 2019. MSC Marc Help Documentation. Non-linear FEA software.
- Matsumura, M., 2015. Wall thinning in carbon steel pipeline carrying pure water at high temperature. *Mater. Corros.* 66 (No. 7), 688–694.
- Miksch, M., Schucktan, G., 1990. Evaluation of Fatigue of Reactor components by on-line monitoring of transients. *Nucl. Eng. Des.* 119, 239–247.
- NEA/OECD, 2014. *Flow Accelerated Corrosion (FAC) of Carbon Steel & Low Alloy Steel Piping in Commercial Nuclear Power Plants*, vol. 6. NEA/CSNI/R. June 2014.
- Netto, T.A., Ferraz, U.S., Botto, A., 2007. On the effect of corrosion defects on the collapse pressure of pipelines. *Int. J. Solid Struct.* 44 (Issues 22–23), 7597–7614.
- Okamoto, K., et al., 2007. A regularization method for the inverse design of solidification processes with natural convection. *Int. J. Heat Mass Tran.* 50, 4409–4423.
- Raju, K.K., Hinton, E., 1980. Non-linear vibrations of thick plates using mindlin plate elements. *Int. J. Numer. Methods Eng.* 15 (2), 249–257.
- Savitzky, A., Golay, E., 1964. Smoothing and Differentiation of data by simplified least squares procedures. *Anal. Chem.* 36 (8), 1627–1639.
- Se-Beom, O., et al., 2019. On-line monitoring of pipe wall thinning by a high temperature ultrasonic waveguide system at the flow accelerated corrosion proof facility. *Sensors*. Apr 19 (8), 1762.
- Taler, J., et al., 2011. Inverse space marching method for determining temperature and stress distributions in pressure components. September. <https://doi.org/10.5772/21614> (Chapter 15).
- Wikstrom, P., et al., 2007. Estimation of the transient surface temperature and heat flux of a steel slab using an inverse method. *Appl. Therm. Eng.* 27, 2463–2472.
- Yun, H., Moon, S.J., Oh, Y.J., 2016. Development of wall-thinning evaluation procedure for nuclear power plant piping - Part 1: quantification of thickness measurement deviation. *Nucl. Eng. Technol.* 48 (No. 3), 820–830.
- Yun, H., et al., 2020. Development of wall-thinning evaluation procedure for nuclear power plant piping - Part 2: local wall-thinning estimation method. *Nucl. Eng. Technol.* 52 (Issue 9), 2119–2129.